Journal of Power Sources 189 (2009) 155–162

Contents lists available at ScienceDirect

Journal of Power Sources

journal homepage: www.elsevier.com/locate/jpowsour

Study of $LiFePO_4$ cathode materials coated with high surface area carbon

Cheng-Zhang Lu [a], George Ting-Kuo Fey [a,*], Hsien-Ming Kao [b]

[a] Department of Chemical and Materials Engineering, National Central University, Chung-Li 32054, Taiwan, ROC
[b] Department of Chemistry, National Central University, Chung-Li 32054, Taiwan, ROC

ARTICLE INFO

Article history:
Received 1 August 2008
Received in revised form
30 September 2008
Accepted 1 October 2008
Available online 17 October 2008

Keywords:
$LiFePO_4$
High surface area carbon
Lithium-ion batteries

ABSTRACT

$LiFePO_4$ is a potential cathode material for 4 V lithium-ion batteries. Carbon-coated lithium iron phosphates were prepared using a high surface area carbon to react precursors through a solid-state process, during which $LiFePO_4$ particles were embedded in amorphous carbon. The carbonaceous materials were synthesized by the pyrolysis of peanut shells under argon, where they were carbonized in a two-step process that occurred between 573 and 873 K. The shells were also treated with a proprietary porogenic agent with the goal of altering the pore structure and surface area of the pyrolysis products. The electrochemical properties of the as-prepared $LiFePO_4$/C composite cathode materials were systematically characterized by X-ray diffraction, scanning electron microscope, element mapping, energy dispersive spectroscopy, Raman spectroscopy, and total organic carbon (TOC) analysis. In $LiFePO_4$/C composites, the carbon not only increases rate capability, but also stabilizes capacity. In fact, the capacity of the composites increased with the specific surface area of carbon. The best result was observed with a composite made of 8.0 wt.% with a specific surface area of 2099 $m^2\,g^{-1}$. When high surface area carbon was used as a carbon source to produce $LiFePO_4$, overall conductivity increased from 10^{-8} to $10^{-4}\,S\,cm^{-1}$, because the inhibition of particle growth during the final sintering process led to greater specific capacity, improved cycling properties and better rate capability compared to a pure olivine $LiFePO_4$ material.

1. Introduction

Over the past few years, a surging demand for portable electronic devices and hybrid electric vehicles has led to the increased production of Li-ion batteries due to their high energy and power density [1]. As is well known, Li-ion batteries involve a reversible intercalation/deintercalation of lithium ions (guest species) into/from a cathode or anode (host matrix) during the discharge/charge process. Since their introduction to the consumer market by Sony Energytec Inc. in 1991, the usable capacity has increased to around 100–150 mAh g^{-1} because structural and chemical stability is a big concern if one extracts more than half the Li from $LiCoO_2$ [2–4]. In addition, cost, safety and environmental concerns associated with meeting the higher energy and power requirements have become key issues. Therefore, the partial or complete replacement of Co with other environmentally benign, cheap elements is one of practical approach. Some of the potential candidate materials are: $LiNiO_2$ [5], $LiMnO_2$ [6], $LiMn_2O_4$ [7] and $LiFePO_4$ [8].

Since Padhi et al. [8] first reported $LiFePO_4$ with an olivine structure in 1997, it has been of great interest because it is environmentally benign, nonhygroscopic, abundant, and low cost in addition to having a theoretical capacity of 170 mAh g^{-1} and good thermal stability [9].

However, because $LiFePO_4$ is an insulating material, it has two fatal disadvantages: low electronic conductivity and slow diffusion of lithium ions across the two-phase boundary, which seriously limits its rate capability [10–12]. Recently, extensive work has been conducted to enhance the electronic conductivity of $LiFePO_4$ by coating it with carbon using either a carbon composite technique, such as a carbon gel or sugar process [13,14] or by doping it with <1.0% Nb^{5+} [13]. These methods have all successfully improved performance, but it has recently been pointed out that small particle sizes adversely affect tap densities [15]. To this end, we have initiated a study on the effect of the structure of residual (less than 10 wt.%) high surface area carbon on the electrochemical performance of $LiFePO_4$ materials. We adopted a solid-state method to obtain fine $LiFePO_4$ powders and mixed the powders with a small amount of high surface area carbon precursor to prepare the carbon-coated $LiFePO_4$ cathode material.

2. Experimental

$LiFePO_4$ was first prepared by a solid-state reaction involving a mixture of iron(II) oxalate (Sigma, 99%), ammonium dihydrogen phosphate (Sigma, 99%), and lithium carbonate (Sigma, 99%) in a

* Corresponding author. Tel.: +886 3 425 7325; fax: +886 3 425 7325.
E-mail address: gfey@cc.ncu.edu.tw (G.T.-K. Fey).

0378-7753/$ – see front matter © 2008 Elsevier B.V. All rights reserved.
doi:10.1016/j.jpowsour.2008.10.015

stoichiometric molar ratio (1:1:1). The precursors were mixed by ball milling in acetone for 3 h. The resulting gel was dried at 333 K in a furnace, thoroughly reground, and heated in purified Ar/H_2 (95:5, v/v) gas for 10 h at 593 K. The decomposed mixture was pressed into pellets and sintered at 873 K in Ar/H_2 (95:5, v/v) gas for 12 h. A grayish black powder of $LiFePO_4$ was obtained. To coat $LiFePO_4$ with carbon, various wt.% (compared to the $LiFePO_4$ to be coated) of high surface area carbon precursors were prepared. $LiFePO_4$ was added to the carbon precursor and was ground by ball milling to make sure that the $LiFePO_4$ powder was totally covered by the carbon precursor. The mixture was finally heated at 873 K in Ar/H_2 (95:5, v/v) for 1 h.

Carbon precursors for this work were synthesized as described below. Good quality dry peanuts (from a local source) were pried open to obtain the shells. The shells were ground into a fine powder. Twenty grams of the powder was mixed with 100 g of a $ZnCl_2$ porogenic agent and stirred well for 24 h. The water in the mixture was allowed to evaporate at 383 K over a period of 4 days. The dry sample was heated at a heating ramp of 10 K min^{-1} in an argon atmosphere and maintained at 423 K for 1 h. Subsequently, the temperature of the sample was raised at a rate of 5 K min^{-1} up to 873 K, at which point it was held again for 1 h. After natural cooling to room temperature, the residue of the $ZnCl_2$ porogenic agent was removed by the treatment in 3 N HCl, followed by a 1 h drying at 463 K. The precise procedure was described in Ref. [16].

Crystal structural analysis of the solid-state synthesized materials was carried out by X-ray diffraction (Siemens D-5000, Mac Science MXP18). The diffraction patterns were recorded between scattering angles of 15° and 80° in steps of 0.05°. Surface composition analysis was obtained by Raman Spectroscopy (ISA T64000) and Total Organic Carbon instrument (OIA, Model Solids-TOC). Raman spectroscopy measurements were carried out at room temperature in ambient atmosphere. The power of the laser beam was adjusted to 50 mW, and the average acquisition time for each spectrum was 5 min. TOC was used to examine the carbon contents in the $LiFePO_4$/C. The morphology of $LiFePO_4$/C composite was observed by Scanning Electron Microscope (SEM; Hitachi S-3500V) and High-Resolution Transmission Electron Microscope (HR-TEM; Jeol TEM-2000FXII). The carbon distribution was confirmed with Energy Dispersive Spectroscopy (EDS) (Energy Dispersive X-ray Spectrometry).

Coin cells of the 2032 configuration were assembled in an argon-filled glove box (VAC MO40-1) in which the oxygen and water contents were maintained below 2 ppm. Lithium metal (Foote Mineral) was used as the anode and a 1 M solution of $LiPF_6$ in EC:DEC (1:1, v/v) (Tomiyama Chemicals) was used as the electrolyte. The cathode was prepared by mixing 85 wt.% $LiFePO_4$-based powders with 10 wt.% carbon black and 5 wt.% polyvinylidene fluoride (PVDF) in *n*-methyl-2-pyrrolidone (NMP) solution. The mixture was pasted on an aluminum foil and dried overnight at 393 K in an oven. The dried coated foil was roller-pressing and circular discs were punching out.

The coin cells were cycled at a 0.2 C rate (with respect to a theoretical capacity of 170 mAh g^{-1}) and 298 ± 0.5 K between 2.8 and 4.0 V in a Maccor 4000 multi-channel battery tester. All electrochemical experiments were conducted at room temperature in a glove-box filled with high purity argon. The conductivity measurements were performed using four-point d.c. methods (Keithly 2400, SR-4 four-point probe).

Phase transitions occurring during the cycling processes were examined by a cyclic voltammetric experiment, performed with a three-electrode glass cell. The working electrode was prepared with the cathode powders as described above, but coated on both sides of the aluminum foil. The cell for the cyclic voltammetric studies was assembled inside a glove box with lithium metal foil serving as both counter and reference electrodes. The electrolyte used was the same as that for the coin cell. Cyclic voltammograms were run on a Solartron 1287 Electrochemical Interface at a scan rate of 0.1 mV s^{-1} between 2.5 and 4.5 V.

Thermal stability analysis was carried out on a PerkinElmer DSC 7 differential scanning calorimetry (DSC) for pristine $LiFePO_4$ and carbon-coated $LiFePO_4$. The measurements were performed in nitrogen atmosphere between 303 and 673 K, at a heating rate of 10 K min^{-1}. The samples for the DSC experiments were prepared as follows. The coin cells were first galvanostatically charged to 4.5 V at a 0.2 C rate and then potentiostated at 4.5 V for 10 h. The coin cells were then opened inside a glove box. The cathode in the coin cell was carefully removed, and the excess electrolyte was wiped with Kimwipes. The cathode was gently scraped from the aluminum current collector, loaded on to an aluminum pan, hermetically sealed, placed in an airtight container, and transferred to the DSC instrument.

BET surface area measurements were carried out on a Micromeritics ASAP 2010 surface area analyzer at 77 K. Prior to the measurements, the as-prepared samples were degassed for 12 h at 523 K under 10^{-6} Torr in order to remove absorbed moisture.

3. Results and discussion

3.1. X-ray diffraction

Fig. 1(a)–(c) shows the XRD patterns of the samples synthesized at 873 K with and without high surface area carbon coating. This olivine structure with PO_4 tetrahedra and distorted FeO_6 octahedra possesses a two-dimensional pathway for lithium ion diffusion [8]. Since most of Fe^{3+} was reduced to Fe^{2+} after calcination at 873 K, no evident impurities such as Fe_2O_3 and $Li_3Fe_2(PO_4)_3$ were detected in both samples.

When the precursor is heated, carbon is generated from the pyrolysis of dry peanut shells in an inert atmosphere, producing

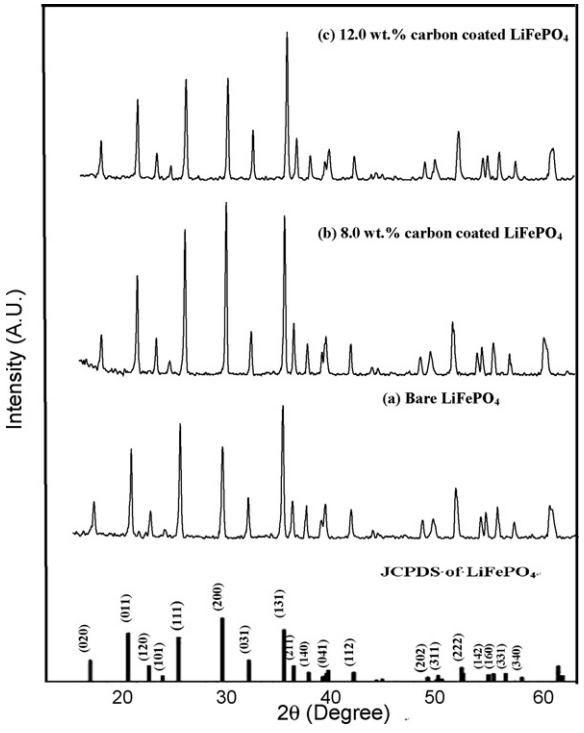

Fig. 1. X-ray diffraction patterns of (a) bare $LiFePO_4$, (b) 8.0 wt.% carbon-coated $LiFePO_4$, and (c) 12.0 wt.% carbon-coated $LiFePO_4$.

a strong reductive atmosphere for the reduction of Fe^{3+} to Fe^{2+}. The high chemical activity of carbon ensures the in situ coating carbon on the surface of fresh formed $LiFePO_4$ particles. It is expected that carbon coating the $LiFePO_4$ crystals will dramatically increase the electronic conductivity of the electrodes, decrease the charge-transfer resistance and facilitate the achievement of good capacities, even at room temperature and relative high rates. However, we cannot find any diffraction peak attributed to carbon in Fig. 1, most likely because there was amorphous or low crystalline carbon in the samples. The cell with $LiFePO_4$/C composite exhibits sharper current peaks, indicating that the composite has improved electrochemical kinetics due to the enhanced electronic conductivity between active cathode grains by carbon. The amorphous and crystalline carbon in the $LiFePO_4$/C composite samples were characterized and discussed later by Raman spectrum analysis.

In some previous reports, the characteristic peaks of Fe_2P impurity was observed in the range $\theta = 45–48^\circ$ in the XRD pattern, when the firing temperature was higher than 1073 K [13]. But in our case, we found no evidence of Fe_2P structure in as-prepared $LiFePO_4$ samples, which may due to the low firing temperature, 873 K. This iron phosphide adopts an hexagonal structure [16]. The presence of either Fe_2P or Fe_2O_3 clusters decreases ionic conductivity so that it degrades both the capacity and cycling rates. It is thus desirable to optimize the preparation of samples to prevent the formation of such clusters.

3.2. Electrochemical behavior

Fig. 2 compares the discharge behavior of pristine $LiFePO_4$, 6, 8, 10 and 12 wt.% of high surface area carbon-coated $LiFePO_4$ between 2.8 and 4.0 V, respectively. In order to study the efficiency of the various wt.% of carbon coating on the cycle performance of Li^+/Li, a preset cut-off value of 80% capacity retention was fixed and calculated with the first-cycle discharge capacity of the respective material.

From Fig. 2, it is observed that the 8.0 wt.% carbon-coated samples exhibited enhanced cycling stability compared to pristine $LiFePO_4$. Based on the cut-off regime, pristine $LiFePO_4$ (108 mAh g^{-1}) could sustain just 10 cycles. In Fig. 2, the number of cycles sustained by 8.0 wt.% high surface area carbon-coated $LiFePO_4$ (138 mAh g^{-1}) was 170 cycles. The 8.0 wt.% coating level may be optimal to form a compact adhesive uniform layer that enhances cycling performance, by protecting the core material from direct contact with the acidic electrolyte, and improves the electron conductivity of $LiFePO_4$. The discharge characteristics of the samples prepared by calcination at different temperatures are plotted as a function of cycle number in Fig. 3. The sample obtained at 823 K delivered a discharge capacity of just 90 mAh g^{-1} in the first cycle, which is very low. The reason for the low capacity is evident from the X-ray diffraction results, which suggest that the $LiFePO_4$/C sample obtained at 823 K is not a completely pure phase. The presence of impurities strongly affects capacity retention. On the other hand, samples calcined at 923 and 1023 K, demonstrated a high first-cycle discharge capacity of 130 and 120 mAh g^{-1}, respectively, but could not sustain extended cycling. The loss of lithium ions during the high temperature calcination process depleted the olivine of lithium ions, resulting in a non-stoichiometric Li—Fe—O phase and poor cycle stability. From Fig. 3, it is observed that the sample heat treated at 873 K for 1 h showed first cycle capacity of 138 mAh g^{-1} and exhibited the best cell performance during extended cycling. Thus, the electrochemical studies concluded that the optimum calcination temperature for the synthesizing $LiFePO_4$ was 600 °C for 1 h. Fig. 4 shows the results of cyclability tests of $LiFePO_4$ electrodes at different charging and discharging rates. Although the specific capacity decreases with increasing charge/discharge rate,

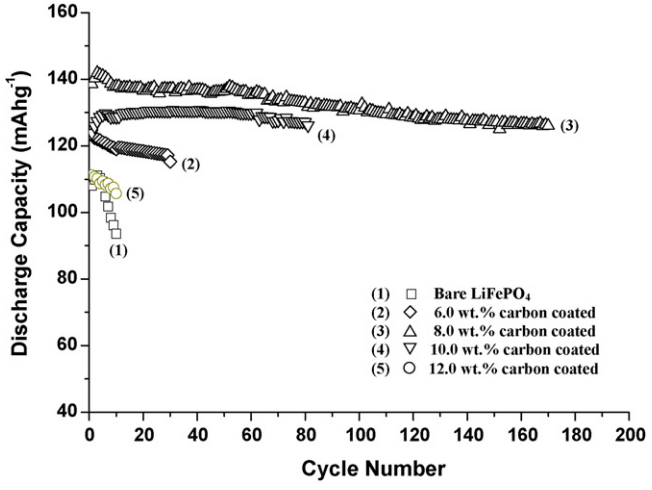

Fig. 2. Discharge curves of the pristine $LiFePO_4$ and the various wt.% carbon-coated. $LiFePO_4$ cathode materials. Charge–discharge: 0.2 C rate between 2.8 and 4.0 V.

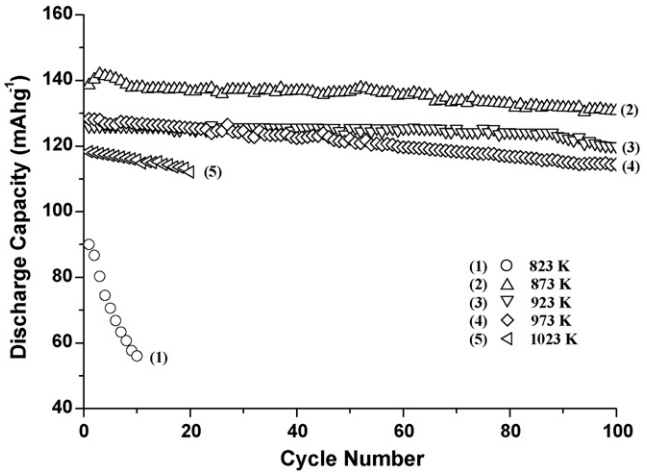

Fig. 3. Discharge curves of the various temperatures synthesized $LiFePO_4$/C cathode materials. Charge–discharge: 0.2 C rate between 2.8 and 4.0 V.

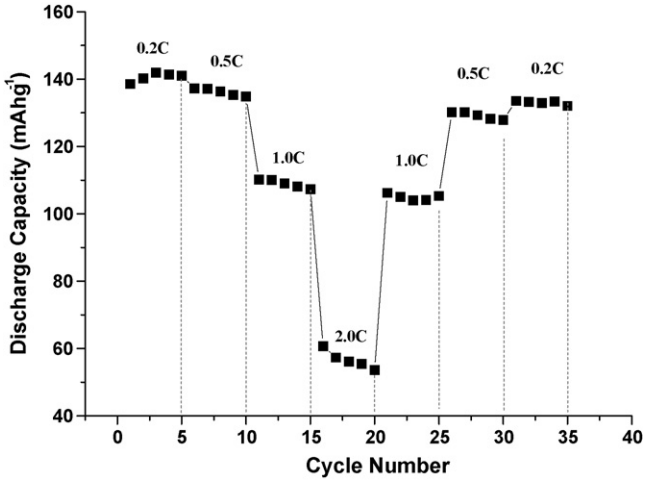

Fig. 4. Cycling behavior of $LiFePO_4$/C cathode materials at different discharge rates. Charge: 0.2 C rate, discharge: 0.2–2.0 C rate between 2.8 and 4.0 V (only discharge curves were shown).

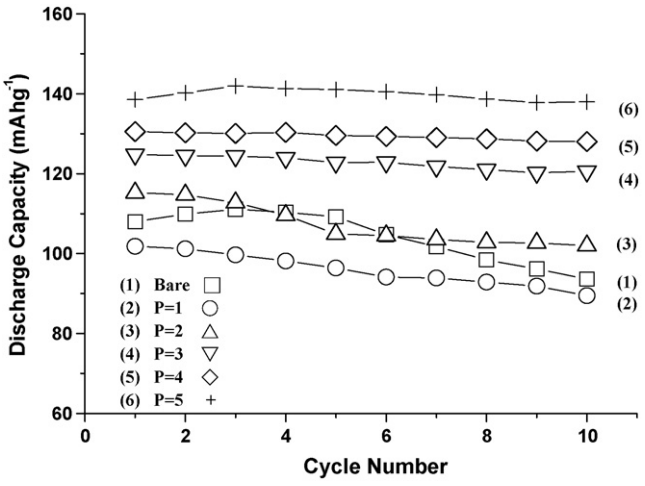

Fig. 5. Discharge curves of $LiFePO_4$/C cathode materials synthesized with different $ZnCl_2$ concentrations. Charge–discharge: 0.2 C rate between 2.8 and 4.0 V.

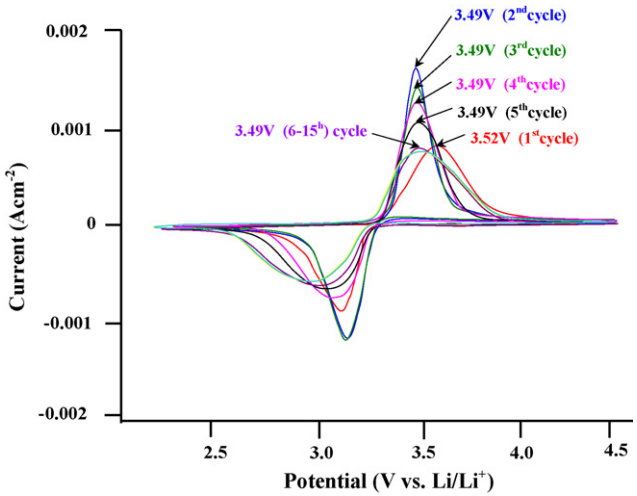

Fig. 6. Cyclic voltammetry of $LiFePO_4$/C cathode at different cycle numbers.

the capacity retention remains very good for all the different rates. Therefore, the high surface area carbon-coated $LiFePO_4$ electrodes demonstrated high capacity and good cyclability. To investigate the effect of the $ZnCl_2$ porogenic agent on the electrochemical performance of $LiFePO_4$/C composites, various p values, $p = 1, 2, 3, 4$, and 5 (where p is weight ratio between $ZnCl_2$ porogenic agent and peanut shells) were used. Fig. 5 shows the $ZnCl_2$ porogenic agent as a function of cycle number. As the $ZnCl_2$ porogenic agent of the composite increased, the specific capacity of the $LiFePO_4$ cathode was found to increase.

It also shows that varying the porogen/peanut shell ratio did not have any significant effect on the elemental compositions of the carbonaceous products [17]. However, the porogen treatment tremendously altered the surface structure. For example, the surface areas of untreated and $p = 5$ treated samples were 31.6 and 2098.9 $m^2\,g^{-1}$, respectively. The corresponding average pore sizes were 17.6 and 33.6 Å. Treatment with the porogen caused a 66-fold increase in the surface area and almost doubled the number of pores to open up. Due to the above factors, it can be deduced that increasing the surface area also increased the capacity of $LiFePO_4$/C composites.

3.3. Conductivity analysis

Table 1 shows the conductivity of the pristine $LiFePO_4$ and the various wt.% high surface area carbon-coated $LiFePO_4$ cathode materials. From the table, increasing the carbon content led to an increase in the conductivity. The conductivity of pristine and 6.0, 8.0, 10 and 12 wt.% high surface area carbon-coated $LiFePO_4$ is 3.97×10^{-8}, 3.45×10^{-4}, 3.70×10^{-4}, 4.63×10^{-4}, and 5.04×10^{-4}, respectively. The result shows the high surface area carbon additive not only can improve the bulk conductivity but also improve the cyclability of the $LiFePO_4$/C composite.

Table 1
Conductivity of the pristine $LiFePO_4$ and various wt.% carbon-coated $LiFePO_4$ cathode materials.

Sample	Thickness of pellet (mm)	Room temperature (295 K)	
		Resistance (kΩ)	Conductivity ($S\,cm^{-1}$)
LFP (0 wt.% HC)	1.06	52316.5	3.97×10^{-8}
LFP (6.0 wt.% HC)	0.77	8.32	3.45×10^{-4}
LFP (8.0 wt.% HC)	0.88	6.78	3.70×10^{-4}
LFP (10 wt.% HC)	0.55	8.67	4.63×10^{-4}
LFP (12 wt.% HC)	0.63	6.95	5.04×10^{-4}

3.4. Cyclic voltammetry

Fig. 6 shows the cyclic voltammogram of the $LiFePO_4$ sample with 8.0 wt.% high surface area carbon at a scanning rate of 0.1 $mV\,s^{-1}$. A pair of redox peaks appears in the CV curves. The sharp oxidation and reduction peaks indicate that strong lithium intercalation and deintercalation reactions occur for as-prepared $LiFePO_4$/C samples. An oxidation peak forms at 3.60 V, and the corresponding reduction peak forms at 3.20 V. The separation between the anodic and cathodic peaks is 0.40 V. From the sixth cycle to the 15th one, the reproducibility of the peaks is representative of the reversibility of the electrode. The peak currents, I_p, during anodic scans at different sweep rates were used to extract the diffusion coefficient, D, of the shuttle molecule using the Randles Sevcik equation $I_p = 2.69 \times 10^5 n^{3/2} A D^{1/2} \nu^{1/2} C$, where A is the electrode area (cm^2), n is the number of electrons involved in the redox process (1 in our case), C is the shuttle concentration ($mol\,cm^{-3}$), ν is the potential scan rate ($V\,s^{-1}$), I_p is in units of amperes, and D is in units of $cm^2\,s^{-1}$ [18]. From the equation, it can be used to extract the diffusion coefficient of the shuttle, D, 1st cycle = 8.82×10^{-8}, 2nd cycle = 3.99×10^{-7}, 3rd cycle = 3.11×10^{-7}, 4th cycle = 2.34×10^{-7}, 5th cycle = 1.98×10^{-7}, 6–15th cycle = 8.18×10^{-8}, respectively. The symmetrical and well-defined CV peaks confirm the outstanding reversibility of the lithium extraction/insertion reactions in the $LiFePO_4$/C composite.

3.5. Raman spectroscopy

The $LiFePO_4$ powders, which range in color from light to dark gray, always contained residual carbon resulting from the combustion of organic moieties in the precursors [19]. Interestingly, performance was not necessarily better with higher carbon contents, although 8.0 wt.% carbon-coated $LiFePO_4$ sample had the highest discharge capacity. These observations indicate that factors besides particle size and carbon content are responsible for variations in the electrochemical characteristics of $LiFePO_4$ powders.

To investigate this phenomenon further, Raman spectroscopy was employed. Fig. 7 shows the Raman spectra of the $LiFePO_4$/C samples sintered with various high surface area carbon contents. Raman spectra consisted of a relatively small band at 940 cm^{-1} attributed to the symmetric PO_4 stretching vibration of $LiFePO_4$,

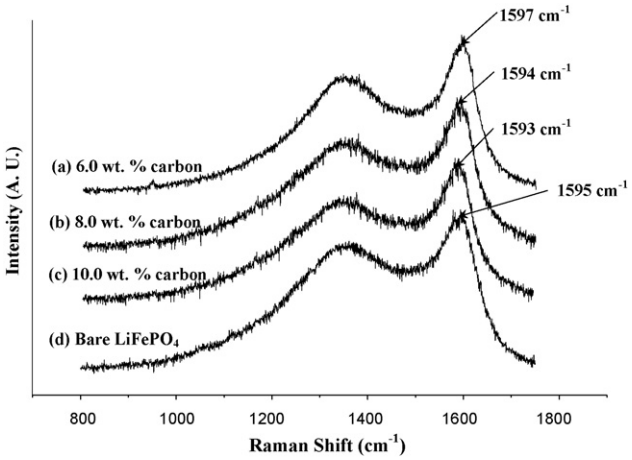

Fig. 7. Raman spectra of the $LiFePO_4$/C samples sintered with various high surface area carbon contents: (a) 6.0 wt.% carbon; (b) 8.0 wt.% carbon; (c) 10 wt.% carbon; (d) bare $LiFePO_4$.

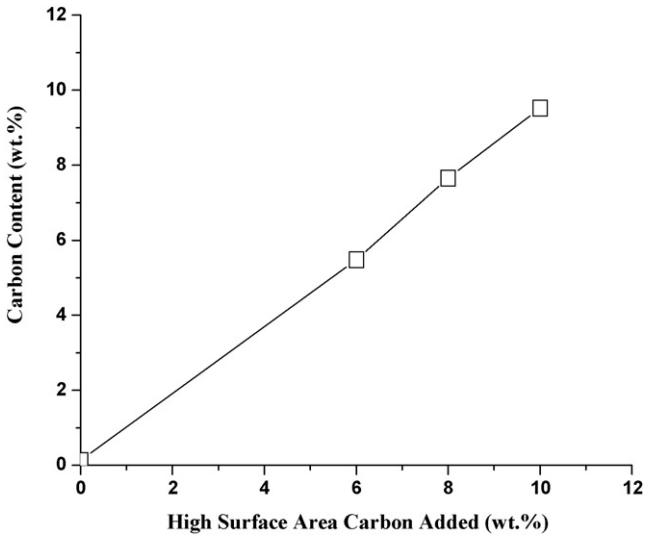

Fig. 8. TOC analysis of high surface area carbon additives.

and intense broad bands at 1350 and 1590 cm^{-1} that can be assigned to the D and G bands of residual carbon, respectively [20]. However, the relative intensities of the D and G bands as well as their shape changed significantly between samples. We noticed that the electrochemical capacity increased for materials with better defined carbon bands. The relative intensity of the D band *vs.* G band is attributed to increased carbon disorder. Doeff et al. [21] reported that decreasing integrated Raman intensity ratio of the D and G bands of carbon will increase the amount of graphene clusters in the structure, leading to improved electronic conductivity of the residual carbon.

The I_D/I_G ratios of the pristine, 6.0, 8.0, and 10.0 wt.% carbon-coated cathodes are 0.962, 0.933, 0.928, and 0.932, respectively, and the electronic conductivities of these samples are 2.94×10^{-5}, 3.45×10^{-4}, 3.70×10^{-4}, and 4.63×10^{-4} S cm^{-1}, respectively. This effect can be explained in terms of the increasing amount of larger graphene clusters in the disordered carbon structure, and consequently, improved electronic conductivity of the carbon deposit. Improved electronic properties of the residual carbon can provide better cell performance. Confirmed by the cell performance, the sample coated by high surface area carbon delivered higher discharge capacities and better rate capability than pristine $LiFePO_4$ cathode.

Thus, the Raman spectra of the samples are consistent with $LiFePO_4$ uniformly coated with highly disordered carbon with a significant contribution from various short-order sp^2- and sp^3-coordinated carbon clusters and functional groups adsorbed on the surface. Higher discharge capacities and better rate capability of $LiFePO_4$ cathodes are directly correlated with increased amounts of sp^2-type carbon domains and decreased levels of disorder in graphene planes.

3.6. TOC analysis

During decomposition and sintering, peanuts shells became carbon that acts as a conductive additive and also controls the particle growth. By changing the amount of carbon, one can control the particle size and conductivity of the material and therefore affect the rate capability of $LiFePO_4$. The effect of the amount of carbon on the properties of materials was therefore investigated. Four samples were made by a solid-state method with 0, 6.0, 8.0, and 10 wt.% so-called high surface area carbon added before heating, respectively. The resultant amount of carbon after heating in these four samples was measured to be about 0.13, 5.48, 7.66, and 9.52 wt.%, respectively by using a Total Organic Carbon Analyzer (TOCOIA, Model Solids-TOC). Fig. 8 shows the carbon contents of the four samples with different quantities of high surface area carbon additive. As the carbon content of the composite increased, the specific capacity of the $LiFePO_4$ phase was found to increase (Fig. 2).

Fig. 2 shows that the capacity at 0.2 C increases dramatically when the amount of carbon increases from 0 to 10 wt.% for cells operated at room temperature. Above 6.0 wt.%, capacity still increases as the amount of carbon increases, but at a much slower rate. A small amount of carbon in the $LiFePO_4$/C composite (less than 10.0 wt.%) can improve the rate capability significantly, which indicates that a high surface area carbon additive can be an effective method for improving the rate capability of $LiFePO_4$. However, even a large amount of added carbon causes a significant decrease in discharge capacity, which may be bad for practical applications. When optimizing the amount of carbon, one must keep an eye on both the rate capability and the tap density. We believe that more effective ways can be found to improve the rate capability of $LiFePO_4$ by using a solid-based method to mix high surface area carbon additives with the raw materials prior to the heating step. If less carbon can be used, the tap density could meet the requirements for practical applications.

3.7. Surface morphology

The sample morphology was observed by a low-vacuum scanning electron microscope (LV-SEM) on a HITACHI (model:S-3500N) equipped with an energy dispersive spectroscopy, which was used to determine the elemental distribution.

For $LiFePO_4$/C composites, carbon distribution and carbon morphology affect its electrochemical performance [22,23]. Fig. 9(a)–(e) shows the SEM images and the corresponding EDS element (P, Fe, C and O) maps of $LiFePO_4$/C composite cathode materials containing 8.0 wt.% high surface area carbon. The $LiFePO_4$/C composite materials show a uniform fine-grained microstructure with particle size in the range of 300–400 nm. Very uniform element distribution was observed for the main elements Fe, P, and O. In addition, the distribution area for high surface area carbon is also homogeneous.

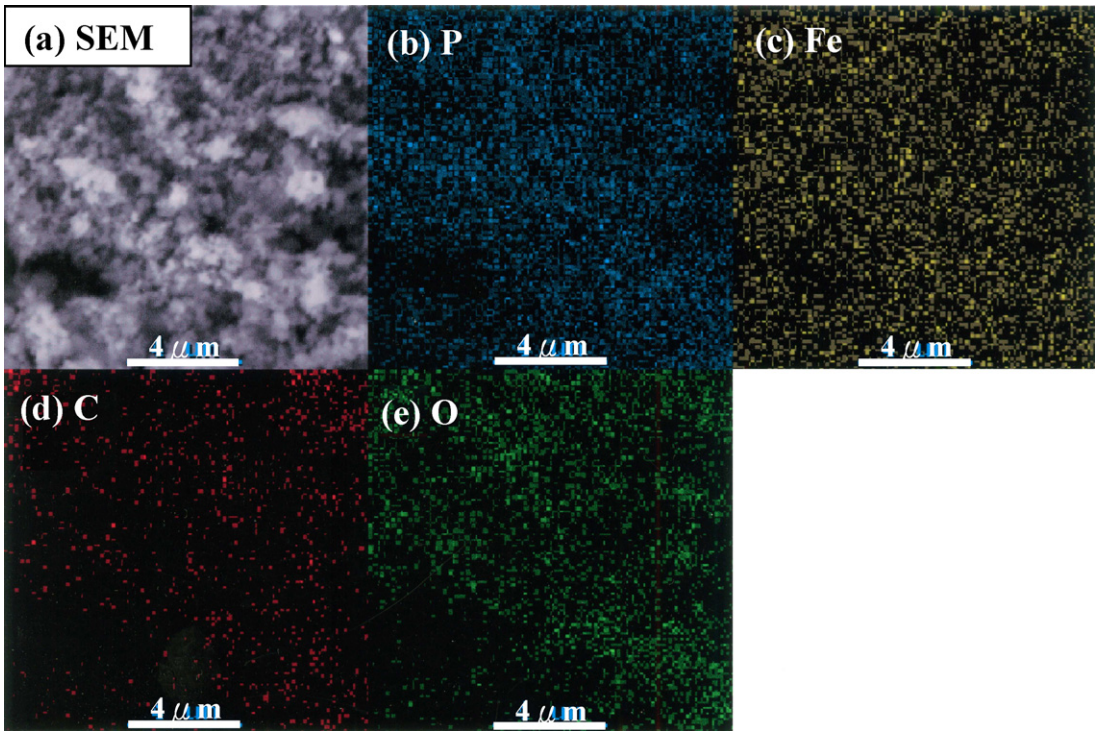

Fig. 9. SEM images and corresponding EDS mappings of $LiFePO_4$/C composite materials containing 8.0 wt.% high surface area carbon. (a) SEM; (b) P; (c) Fe; (d) C; (e) O.

3.8. TEM/EDX analysis

In order to confirm the prepared powder covered by carbon, TEM and SAED observations were carried out and the results are shown in Fig. 10. The high surface area carbon-containing $LiFePO_4$ powders were homogeneous and had a smaller particle size of about 300–500 nm of $LiFePO_4$ (Fig. 10(a)). To confirm how the carbons are distributed with the $LiFePO_4$ powder, a part of the $LiFePO_4$ powder

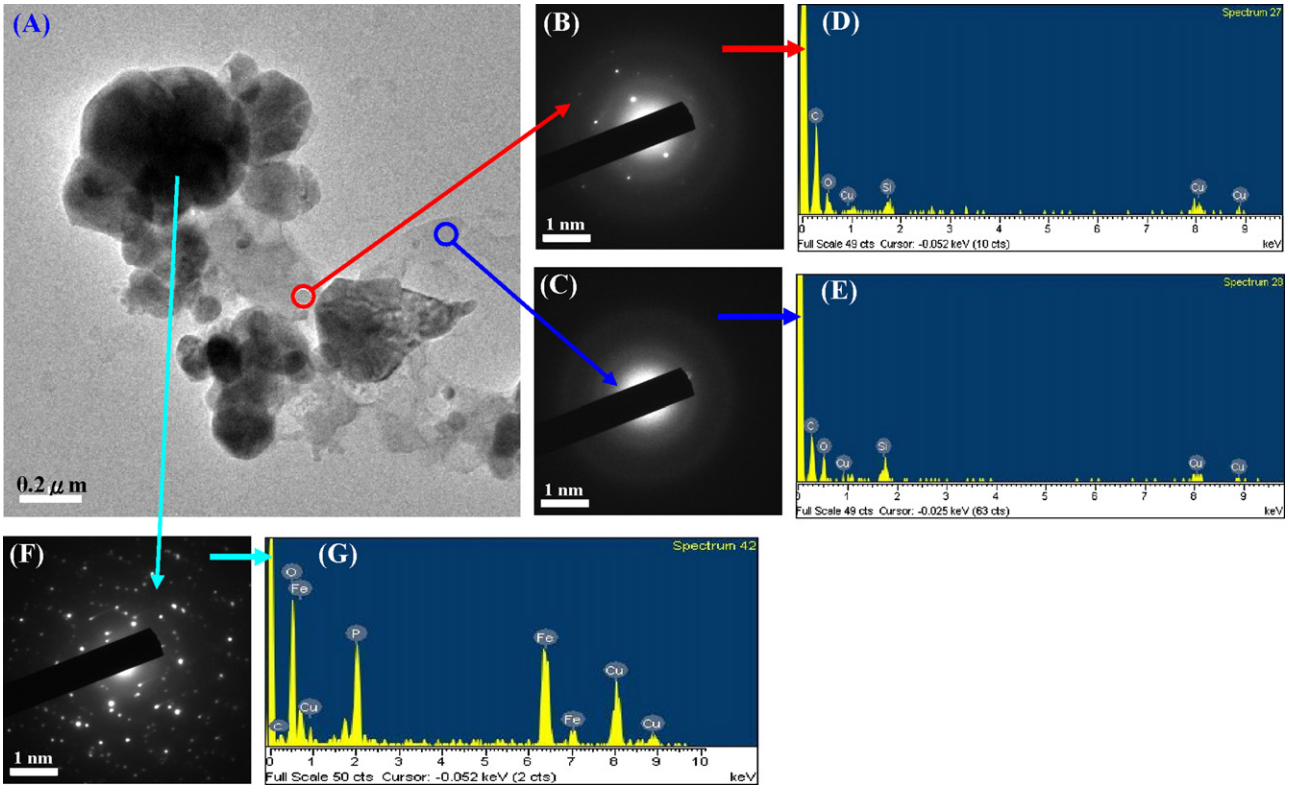

Fig. 10. TEM/EDX analysis of $LiFePO_4$/C cathode.

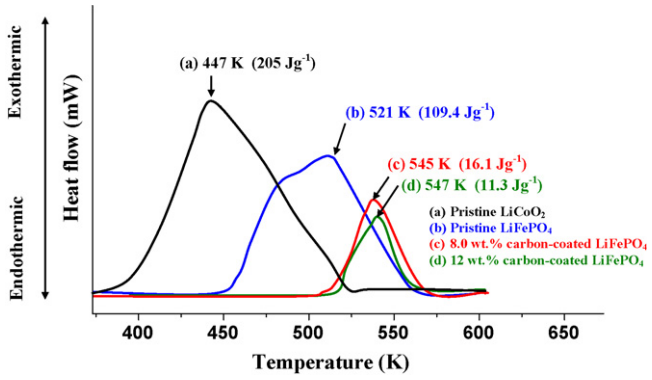

Fig. 11. DSC analysis of $LiCoO_2$ and $LiFePO_4$/C samples.

which contains 8.0 wt.% high surface area carbon was magnified as shown in Fig. 10. It is clear from the image that the surface of the $LiFePO_4$ powder is modified by carbon. This means that the high surface area carbons (marked primary particles by arrows) are agglomerated and finely composed of $LiFePO_4$. The particle size of carbon is measured to be less than 50 nm. Therefore, hereafter the carbon-containing $LiFePO_4$ powder is called a $LiFePO_4$/C composite. Remarkably, Fig. 10(b) region is graphite, and Fig. 10(c) region is amorphous carbon. The amorphous and graphitic carbon were coexisted. On the other hand, in Raman spectra, the I_D/I_G ratio showed above are both smaller than unity, showing that there are more than half of useful carbon graphitized carbon coated on the $LiFePO_4$ during the pyrolysis step. This result also consists with the existence of crystalline carbon which were analyzed by the TEM/SAED/EDX techniques.

3.9. Thermal analysis

In order to improve the safety of Li-ion batteries, it is necessary to understand their thermal stability and heat generation from decomposition or exothermic reactions of the materials within the cell. Fig. 11 shows the DSC curves for overcharged pristine $LiCoO_2$, pristine $LiFePO_4$, 8.0 and 12.0 wt.% high surface-area carbon-coated $LiFePO_4$ samples, respectively. It was observed that the onset temperatures (T_o) of $LiCoO_2$, $LiFePO_4$, 8.0 and 12.0 wt.% high surface area carbon-coated $LiFePO_4$ samples were around 383, 452, 512, and 520 K, respectively. The decomposition temperatures (T_d) were around 447, 521, 545, and 547 K, respectively. The $LiFePO_4$ samples showed a higher onset temperature and decomposition temperature than pristine $LiCoO_2$. For the carbon-coated samples of $LiFePO_4$, total heat evolution was just around 20 J g^{-1}. In contrast, much greater heat evolution with significant oxygen loss was observed in charged pristine $LiCoO_2$ and $LiFePO_4$. For instance, the overall heat generation of the fully charged $LiCoO_2$ and $LiFePO_4$ was 205 and 109 J g^{-1}, respectively. Therefore, it can be concluded that $LiFePO_4$ and its carbon-coated samples have better thermal safety characteristics than a pristine $LiCoO_2$ cathode material. The extremely stable nature of the olivine structure will produce batteries with high tolerance to extreme temperatures.

3.10. Surface area analysis

The BET surface area of the as-prepared $LiFePO_4$/C samples at various carbon content is shown in Table 2. Table 2 summarizes the relationship between TOC, capacity, conductivity and specific surface area results of carbon-coated samples. It shows that capacity of the composites has no obvious correlation with the specific surface area, carbon content, and conductivity. However, capacity increases with specific surface area of carbon-coated $LiFePO_4$ samples to higher levels than the pristine one. The composite with 8.0 wt.% high surface area carbon, having a specific surface area of 111.9 m^2 g^{-1}, shows the highest initial discharge capacity of 138 mAh g^{-1}. When increasing the carbon content of $LiFePO_4$/C composites, the specific surface area of materials also increased. It was observed that the surface area of the pristine, 6, 8, 10, and 12 wt.% carbon-coated $LiFePO_4$ samples was 14, 91, 112, 142 and 170 m^2 g^{-1}, respectively. These results demonstrated that high surface area carbon can improve the specific area of $LiFePO_4$/C composites. Fig. 1 compares XRD patterns of $LiFePO_4$/C composites with various carbon contents. $LiFePO_4$/C composites with high surface area carbon display sharper diffraction peaks [24], which leads us to recommend the use of high surface area carbon in the preparation of $LiFePO_4$/C composites.

Table 2
BET analysis of the pristine $LiFePO_4$ and various wt.% carbon-coated $LiFePO_4$ cathode materials.

Sample	TOC (wt.%)	BET surface area (m^2 g^{-1})	1st d.c. (mAh g^{-1})	Conductivity (S cm^{-1})
Pristine LFP	0.13	13.7445	108	3.97×10^{-8}
LFP + 6.0 wt.% HSAC	5.48	91.4824	123	3.45×10^{-4}
LFP + 8.0 wt.% HSAC	7.66	111.9023	138	3.70×10^{-4}
LFP + 10.0 wt.% HSAC	9.52	142.5012	124	4.63×10^{-4}
LFP + 12.0 wt.% HSAC	11.63	170.3214	112	5.04×10^{-4}
HSAC	–	2099	–	–

4. Conclusions

A high surface area carbon additive prepared using a solid-state method was found to be an effective technique for synthesizing an olivine phase of $LiFePO_4$ with good cyclability. A highly pure phase with increased crystallinity was obtained at a temperature as low as 873 K. Galvanostatic cycling studies showed the optimum heat treatment procedure was 1 h calcination at 873 K where the sample sustained 170 cycles between 2.8 and 4.0 V at a charge–discharge rate of 0.2 C. We have shown that carbon as a conductive additive plays an important role in improving performance, since it increased the utilization of active material and the electrical conductivity of the electrode. In the case of a $LiFePO_4$/C composite (8.0 wt.% high surface area carbon) synthesized by adding peanut shell during the initial heating of the reactants, the high surface area carbon precursor was added before heating, so the particles were uniform and well-coated by carbon and the overall conductivity increased from 10^{-8} to 10^{-4} S cm^{-1}, since particle growth was prevented during the final sintering process. These characteristics apparently promote good cycle capacity and rate capability.

References

[1] Du Pasquier, F. Disma, T. Bowmer, A.S. Gozdz, G. Amatucci, J.M. Tarascon, J. Electrochem. Soc. 145 (1998) 472.
[2] Y. Sakurai, H. Arai, S. Okada, J. Yamaki, J. Power Sources 68 (1997) 711.
[3] R. Kanno, T. Shirane, Y. Kawamoto, Y. Takeda, M. Takano, M. Ohashi, Y. Yamaguchi, J. Electrochem. Soc. 143 (1996) 2435.
[4] Y.S. Lee, C.S. Yoo, Y.K. Sun, K. Kobayakawa, Y. Sato, Electrochem. Commun. 4 (2002) 727.
[5] H. Arai, S. Okada, Y. Skurai, J.I. Yamaki, Solid State Ionics 95 (1997) 275.
[6] A.J. Paterson, A.R. Armstrong, P.G. Bruce, J. Electrochem. Soc. 151 (2004) A1552.
[7] S. Neito, S.B. Majumder, R.S. Katiyar, J. Power Sources 136 (2004) 88.
[8] A.K. Padhi, K.S. Nanjudaswamy, J.B. Goodenough, J. Electrochem. Soc. 144 (4) (1997) 1188.
[9] J.B. Lu, Z.T. Zhang, Z.L. Tang, Rare Met. Mater. Eng. 33 (2004) 679.
[10] A.S. Andersson, B. Kalska, L. Haggstrom, J.O. Thomas, Solid State Ionics 130 (2000) 41.
[11] A. Yamada, S.C. Chung, K. Hinokuma, J. Electrochem. Soc. 148 (3) (2001) A224.
[12] N. Ravet, Y. Chouinard, J.F. Magnan, S. Besner, M. Gauthier, M. Armand, J. Power Sources 97–98 (2001) 503.

[13] S.Y. Chung, J.T. Bloking, Y.M. Chiang, Nat. Mater. 1 (2002) 123.
[14] S. Franger, C. Bourbon, F. Gras, J. Electrochem. Soc. 151 (7) (2004) A1024.
[15] Z. Chen, J.R. Dahn, J. Electrochem. Soc. 149 (2002) A1184.
[16] B. Carlsson, M. Gölin, S. Rundqvist, J. Solid State Chem. 8 (1970) 57.
[17] G.T.K. Fey, D.C. Lee, Y.Y. Lin, T. Prem Kumar, Synth. Met. 139 (2003) 71.
[18] J.R. Dahn, J. Jiang, L.M. Moshurchak, M.D. Fleischauer, C. Buhrmester, L.J. Krausec, J. Electrochem. Soc. 152 (6) (2005) A1283.
[19] M.M. Doeff, Y. Hu, F. McLarnon, R. Kostecki, Electrochem. Solid State Lett. 6 (2003) A207.
[20] S.W. Song, R.P. Reade, R. Kostecki, K.A. Striebel, J. Electrochem. Soc. 153 (1) (2005) A12.
[21] M.M. Doeff, J.D. Wilcox, R. Kostecki, G. Lau, J. Power Sources 163 (2006) 180.
[22] R. Dominko, M. Gaberscek, J. Drofenik, M. Bele, S. Pejovnik, J. Jamnik, J. Power Sources 119–121 (2003) 770.
[23] P. Herle, B. Ellis, N. Coombs, L.F. Nazar, Nat. Mater. 3 (2004) 147.
[24] S.S. Zhang, J.L. Allen, K. Xu, T.R. Jow, J. Power Sources 147 (2005) 234.